# Kinetics of Dibenzylether Hydrothermolysis in Supercritical Water

**Guillermo González and Daniel Montané**
Dept. of Chemical Engineering, ETSEQ, Rovira i Virgili University, Av. Països Catalans,
26. E-43007 Tarragona (Catalunya), Spain

*DOI 10.1002/aic.10362*

*The kinetics of dibenzylether (DBE) hydrothermolysis in hot compressed water has been investigated in a continuous tubular reactor system at a pressure from 225 to 362 bar, temperature from 325 to 390°C, and a constant water load of* $\Theta_W = 100\ mol_{water}/mol_{DBE}$*. Thermal scission of DBE yielded equimolar amounts of benzaldehyde and toluene; the rate constant in supercritical water decreased with water density showing that the volume of activation was positive, as expected for an unimolecular scission reaction. Benzyl alcohol was produced by DBE reversible hydrolysis catalyzed by free protons from water dissociation. Density and dielectric constant of water decreased the rates of hydrolysis and DBE formation, which means that the transition state complex has a positive volume of activation, and a lower dipolar moment than the reactants. As the dielectric constant raises the reaction rates are lowered, but the equilibrium shifts toward the formation of benzyl alcohol, which is more polar than DBE. The low dipole moment of the transition state complex was further supported by the negative effect of the ionic strength on the rate constant for DBE hydrolysis.* © 2005 American Institute of Chemical Engineers *AIChE J,* 51: 971–981, 2005
*Keywords: hydrothermal reactions; supercritical water; hydrolysis; kinetics.*

## Introduction

Lignocellulosic biomass is a renewable resource that offers a high potential for the production of energy carriers and chemicals, and multiple applications are currently under study in these fields. Lignin is the second most important polymer among the constituents of lignocellulosic biomass. In its native state it is a random three-dimensional (3-D) polymer formed by phenyl-propane monomers. Lignin is obtained as a byproduct in the chemical pulp industry, and it is mainly used as fuel to provide steam for the pulping plant, but the production of derivatives from lignin is envisaged as a key factor for developing chemicals from renewables industrially. The use of sub- and supercritical water (SCW) as a reaction medium offers a variety of possibilities for chemistry because of the strong variations in density, the dielectric constant and the ionic product of water around the critical point.[1-3] Biomass processing in supercritical water has attracted considerable attention as a method for obtaining liquid and gaseous fuels and energy carriers.[4-11] Homogeneous and heterogeneous catalysts have also been added to promote the gasification of cellulose and lignocellulosic biomass in SCW at lower reaction temperatures. Nickel-based catalysts[12] and activated carbon[13] have been tested as heterogeneous catalysts, while KOH and $K_2CO_3$ have been shown to act as homogeneous catalysts for gasifying glucose and lignin model compounds.[14] Reactions of lignin model compounds in supercritical water have been studied in several articles.[15-17] Studies on the hydrothermal reactions of aromatic dimers that contain ether linkages representatives of lignin structure like diphenylether[4,18] and dibenzylether[19,20] have shown the coexistence of the hydrolysis and pyrolysis pathways, and the influence of water density on the dominance of one reaction path or the other. These studies covered a narrow range of temperature and were performed at constant

---

Correspondence concerning this article should be addressed to D. Montane at dmontane@etseq.urv.es

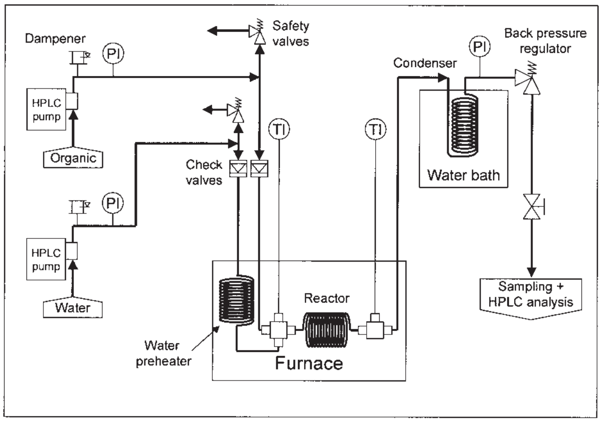

**Figure 1. Tubular reactor unit.**

density. Furthermore, the effect of the concentration of free protons from water dissociation was not accounted for in the analysis of the data, but this is a key aspect for the correct interpretation of reactions, such as the hydrolysis of ethers[4,21-23] and esters[24] in supercritical water, or the dehydration of alcohols[25,26] at subcritical conditions. In this article, we have selected dibenzylether (DBE) as a model compound representative of the ether linkages in lignin. We have studied the hydrothermal conversion of DBE in high- temperature water and the selectivity toward the main reaction products systematically. The experimental study has been performed in a continuous flow reactor at a pressure from 225 to 362 bar, temperature from 325 to 390°C, and at short residence time to minimize secondary reactions of the primary products. A kinetic model that accounts for the effect of water dissociation and the influence of the concentration of protons on the reaction rates has been developed, and the rate constants have been estimated from the experimental data.

## Materials and Method

### *Reactor system*

The hydrothermolysis experiments were developed in the continuous tubular reactor system seen in Figure 1, which has been described in detail elsewhere.[27] Dibenzylether (DBE) and water were pumped separately with two HPLC pumps (0.1-10 mL/min). Water was deoxygenated by bubbling nitrogen into the bottle and then it was degassed in an ultrasound bath. Water was kept under a nitrogen atmosphere along the experiment by purging the gas inside the bottle with a small flow of nitrogen to prevent air to enter. The bottles containing the feeds were placed on balances (± 0.01 g) that were connected to a data acquisition system. The instantaneous mass flow rates fed to the reactor were calculated online to monitor their stability along the experiment. The use of balances provided an efficient way for determining the amount of water and DBE feed to the reactor over a certain period of time with the highest accuracy, thus lowering the uncertainties on the mass and carbon balances. The flow of water was preheated in a coil, and the flow of DBE was fed through a short capillary tube to minimize thermal degradation and mixed with the preheated water to obtain the desired concentration of dibenzylether at the reactor inlet. Two reactors 1 and 4 m long were used, depending on the range of residence times of interest. The temperatures at the inlet and outlet of the reactor were measured with type K thermocouples. The water preheater and the reactor were made of Hastelloy C-276, and the system was mounted inside an electrical furnace to achieve isothermal operation. The reactor effluent was cooled to room- temperature in a coil submerged in a water bath, and the pressure inside the reactor was adjusted and maintained with a back pressure regulator. The experiments were performed by setting the water flow rate, pressurizing the reactor and heating the system to the desired temperature. When temperature and pressure were stable, the feed of DBE was initiated with the other HPLC pump and the reactor was operated for 15 min before the first sample of the product was collected. This time was at least six times higher than the total residence time of the mixture in the system (reactor + cooling tube), and it was established that it was enough to ensure that the reactor had reached steady state by analyzing several samples of the product. Normally, four samples of the reactor effluent were then collected along 1 h, and their were analyzed separately to calculate the average molar flows of the products and their confidence interval at the 95% probability. The mixture of water, nonreacted DBE and reaction products formed two partially miscible phases at room-temperature and a specific procedure was developed to obtain representative samples. Samples of the reactor effluent were collected for 2 to 5 min (depending on the total flow rate) in a volumetric flask and the sample was weighted to check the total mass balance of the system. Acetonitrile was then added to adjust the total volume. The amount of acetonitrile was large enough for the mixture to form a single liquid phase. The samples were then filtered in a 20 $\mu$m syringe filter and analyzed by isocratic HPLC as described later.

### *Analytical methods*

HPLC analysis was carried out in an Agilent series 1,100 chromatograph equipped with an UV-visible diode array detector. Separation was performed in a Supelco LC-8 58220-U octylsilyl column using 1.0 mL/min of water:acetonitrile (60: 40). Standards of DBE (>98%, Fluka), benzyl alcohol (>99%, Aldrich), toluene (>99%, Fluka), benzaldehyde (>99%, Aldrich) and benzene (>99.9%, Aldrich) were analyzed and their UV-spectra recorded. The peaks observed during the analysis of the reaction products were identified by the retention time and the match between the their UV-spectra and those of the standards.

## Results and Discussion

### *Hydrothermolysis of dibenzylether and reaction products*

The products from the hydrothermolysis of dibenzylether (DBE) were benzyl alcohol, toluene and benzaldehyde. Very minor amounts of benzene were also detected at high temperature and long residence time. Figures 2 and 3 show the yields of the reaction products for the experiments performed at subcritical temperature and pressures of 250, 275 and 300 bar, using a water to DBE molar ration ($\Theta_w$) of 100 $\mathrm{mol_{water}/mol_{DBE0}}$. Yield was defined as the ratio $F_j/F_{DBE0}$, where $F_j$ is the molar flow for the $j$ species and $F_{DBE0}$ is the molar flow of DBE at the reactor inlet. Error bars are the confidence intervals of the average values at the 95% probability level. Reactions

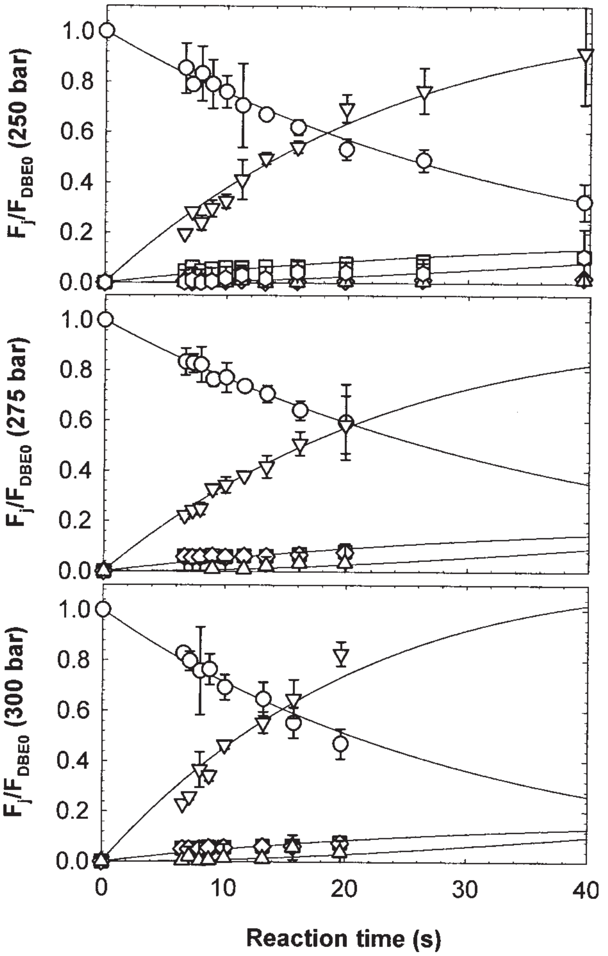

**Figure 2. Hydrothermolysis of DBE at $\Theta_W = 100\ \mathrm{mol_{water}}/\mathrm{mol_{DBE}}$.**

Fractional yields of reaction products at 325°C and 250, 275 and 300 bar (DBE ○; BAL ▽; BZA □; TOL ◇; DEG △).

involved in the hydrothermolysis of DBE were fast at those conditions. For example, a conversion of DBE close to 38% was obtained at 325°C and 250 bar in only 16 s of residence time. The main reaction product was benzyl alcohol with a yield of 0.54 mol/mol$_{DBE0}$, while toluene (0.064 mol/mol$_{DBE0}$), and benzaldehyde (0.066 mol/mol$_{DBE0}$) were also identified as minor products. Conversion to unidentified degradation and condensation products was 4.3% of the DBE (molar basis). When pressure was augmented to 300 bar conversion of DBE grew, and the yield of benzyl alcohol was slightly higher. After 16 s of residence time the DBE conversion was around 45% and the yields of benzyl alcohol, benzaldehyde and toluene were 0.65, 0.065 and 0.063 mol/mol$_{DBE0}$, with 5.8% of the DBE converted to unidentified products. Analysis of the data in Figure 3 for the isothermal series at 350°C shows the same trends for the influence of pressure. At 250 bar and a residence time of 15s DBE conversion was 54% and the yields of benzyl alcohol, benzaldehyde and toluene were 0.79, 0.090 and 0.086 mol/mol$_{DBE0}$. At 300 bar conversion raised to 59%, and the yields were 0.83, 0.102 and 0.105 mol/mol$_{DBE0}$ for benzyl alcohol, benzaldehyde and toluene. The unidentified products accounted for 5.9% at 250 bar and 7.2% at 300 bar. In conclusion, rising the pressure at constant temperature intensifies the rate of benzyl alcohol formation, but has only a slight effect on selectivity since the rates of toluene and benzaldehyde formation also increase.

The influence of pressure on DBE conversion and reaction rates was more important above the critical temperature of water. Figure 4 shows the results obtained for the isothermal series performed at 375°C and pressures of 225, 250, 275, 300 and 325 bar. These experiments show higher dispersion because they were performed close to the critical temperature of water, where small fluctuations in temperature and pressure have a large impact on the properties of water. Pressure decreases the rate of DBE hydrothermolysis and the yields of benzaldehyde, toluene and degradation products, but increases the yield of benzyl alcohol. Selectivity toward the formation of benzyl alcohol (BAL) is shown in Figure 5 for selected pressures. It was calculated as the ratio between the molar flow of benzyl alcohol and that of benzaldehyde, toluene and degradation products, $F_{BAL}/(F_{TOL} + F_{BZA} + F_{DP})$. The 95% confidence intervals (error bars) were calculated by error propagation from the errors determined previously for the molar flow rates. Increasing pressure alters the selectivity toward the formation of benzyl alcohol over secondary products. The experiments at 275 and 300 bar were extended to longer residence times to reach higher conversions of DBE. It is observed that at 275 bar the fractional yield of DBE tends to stabilize at 0.02 mol/

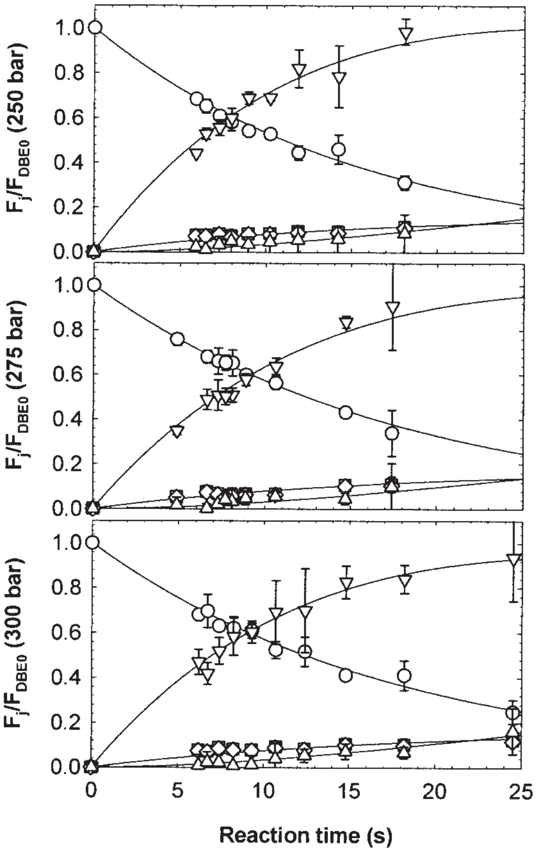

**Figure 3. Hydrothermolysis of DBE at $\Theta_W = 100\ \mathrm{mol_{water}}/\mathrm{mol_{DBE}}$.**

Fractional yields of reaction products at 350°C and 250, 275 and 300 bar (DBE &CIR;; BAL ▽; BZA □; TOL ◇; DEG △).

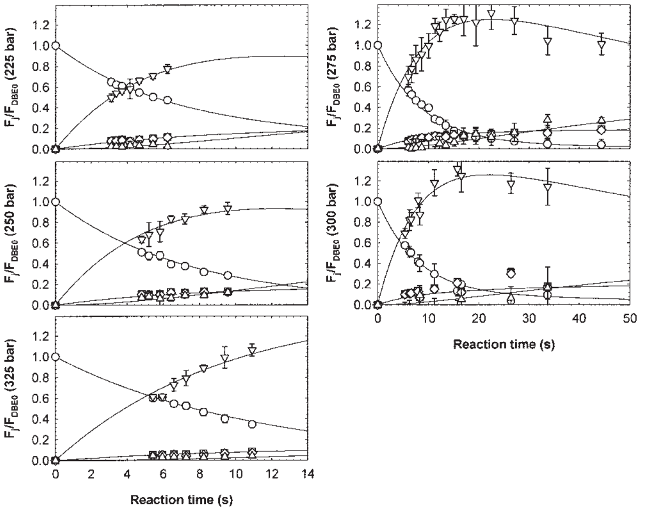

**Figure 4. Hydrothermolysis of DBE at $\Theta_W = 100$ mol$_{water}$/mol$_{DBE}$.**

Fractional yields of reaction products at 375°C and 225, 250, 275, 300 and 325 bar (DBE ○; BAL ▽; BZA □; TOL ◇; DEG △).

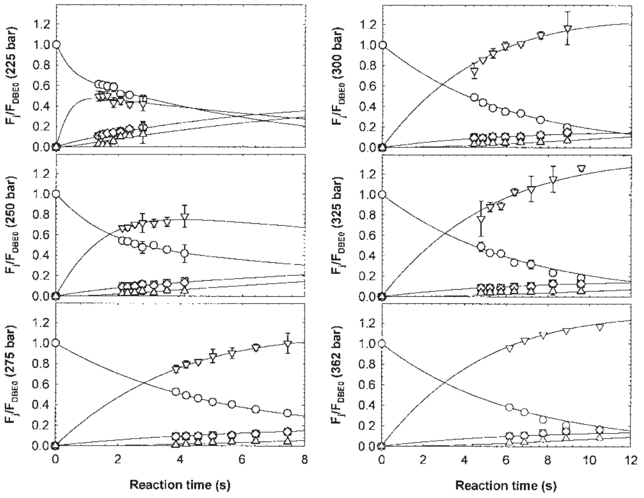

**Figure 6. Hydrothermolysis of DBE at $\Theta_W = 100$ mol$_{water}$/mol$_{DBE}$.**

Fractional yields of reaction products at 390°C and 225, 250, 275, 300, 325 and 362 bar (DBE ○; BAL ▽; BZA □; TOL ◇; DEG △).

mol$_{DBE0}$ without achieving complete conversion. This suggests an equilibrium for DBE hydrolysis to benzyl alcohol, in agreement with previous works.[20] Analysis of the data also shows that toluene and benzaldehyde are always present in equimolar amounts, even at the longer reaction time, and that their concentration levels off at a nearly constant value when DBE has been extensively converted. This indicates that they are formed directly by the cleavage of the ether bond in DBE and do not react significantly further, at least for the interval of reaction time covered in this study. This experiment also shows that the amount of unidentified products grows at the same rate as benzyl alcohol disappearance. Further evidence of the equilibrium between DBE and benzyl alcohol is obtained from the isothermal series performed at 390°C and pressures from 225 to 362 bar (Figure 6). At 225 bar a maximum yield of benzyl alcohol of 0.5 mol/mol$_{DBE0}$ was rapidly obtained in less than 2 s, while DBE conversion was around 40%. At a longer reaction time the concentrations of DBE and benzyl alcohol decreased steadily, while the concentration of toluene, benzaldehyde and the amount of degradation products raised continuously. Lower reaction rates were observed at 250 bar, although the yield of benzyl alcohol was higher than at 225 bar and those of toluene, benzaldehyde, and degradation products lower. The same trend of higher yields of benzyl alcohol and lower yields of toluene, benzaldehyde and degradation products was observed at pressures up to 362 bar. Figure 5 shows the selectivity toward benzyl alcohol at 225, 250, 300 and 325 bar. Selectivity increases with reaction pressure and a poor selectivity is obtained at the lower pressures since they favor the formation of benzaldehyde and toluene over benzyl alcohol.

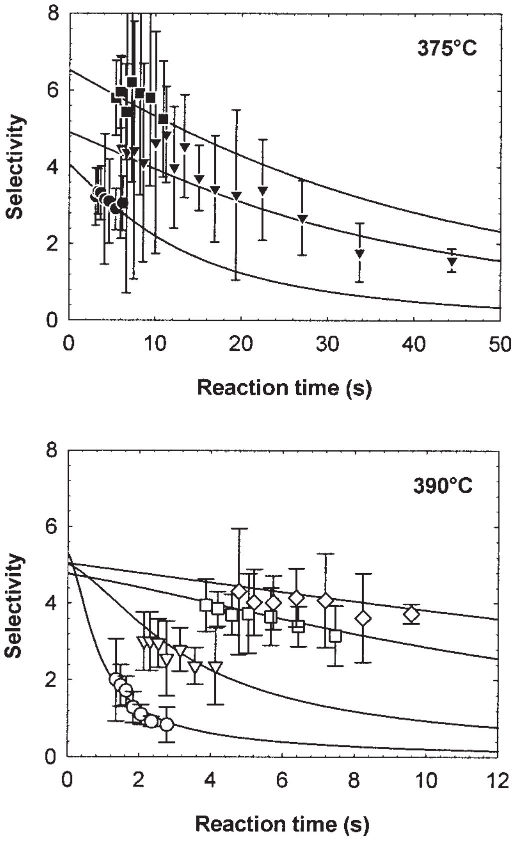

**Figure 5. Selectivity towards benzyl alcohol formation at 375°C (225 bar ● 275 bar ▼; 325 bar ■) and 390°C (225 bar ○; 250 bar ▽; 275 bar □; 325 bar ◇).**

The qualitative interpretation of the experimental data indicates that DBE hydrothermolysis proceeds through two competitive parallel reactions: thermal cleavage of the ether bond to form toluene and benzaldehyde and hydrolysis to form benzyl alcohol, which is further converted to unidentified degradation and/or condensation products as in Figure 7. This is basically a simplified of the reaction pathway proposed by Funazukuri et al.[20] In our case we have assumed that toluene and benzaldehyde are stable at the short reaction times that we have studied

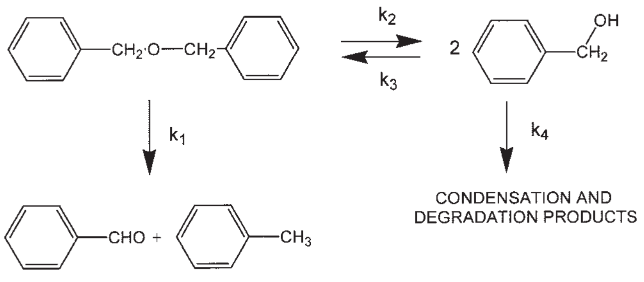

**Figure 7. Reaction pathways for DBE conversion under hydrothermal conditions.**

since they are always detected in equimolar amounts regardless of the reaction conditions and time. Hence, reactions like the formation of benzene, toluene and benzyl alcohol from benzaldehyde, and the degradation of toluene and benzaldehyde to other products have been not included in the model. It was observed that the closure in the balance of aromatic rings decreased at the same rate as benzyl alcohol disappearance, although it was not possible to identify these products nor quantify them. We assumed that the degradation products were formed exclusively from benzyl alcohol, and the amount of degradation products was calculated by difference from a balance of aromatic rings. This means that differences in the mass balance caused by random errors in the feeds flow rate, and the analysis of the reaction products are accounted as degradation of benzyl alcohol. The use of balances to measure the mass flow rates of DBE and water ensured reproducibility and precision in the reactor feed. Experiments conducted at low-temperature demonstrated mass balance closures between 98 and 102% for DBE. Thermal degradation of DBE in the capillary tubing of the feed line is another factor that may contribute to imprecision in the mass balance. Thermal degradation of DBE produces toluene and benzaldehyde as main primary products, together with small amounts of benzene, aromatic dimmers formed from toluene, gases and a char residue.[20,28] Extended thermal degradation of DBE in the capillary line will generate high concentrations of toluene and benzaldehyde in the reactor feed, but the trends observed in the experimental data suggest that their concentration was practically zero at the reactor inlet ($\tau = 0$). The residence time for DBE in the high-temperature section of the capillary line was calculated to be around 10% of the residence time in the reactor tube, which minimized the possibility of a high degree of thermal degradation. Some char formation was observed only for the experiments at 390°C, although the amount was too small to be measured. It was detected because it accumulated in the back pressure regulator and caused malfunction after a several hours of continuous operation of the reactor. We think that it is more likely that this solid product was formed by condensation reactions inside the reactor rather than by thermal degradation of DBE in the feed line. The appropriateness of these assumptions are supported by the good concordance between the experimental data and the kinetic model developed from this reaction scheme in all the experiments we performed.

### *Kinetics of dibenzylether conversion*

Individual mass balances for dibenzylether (DBE), benzyl alcohol (BAL), benzaldehyde (BZA), toluene (TOL), and degradation products (DP) were developed for the tubular reactor assuming isothermal and isobaric operation. A plug flow behavior for the reactor and instantaneous mixing and homogenization of water and DBE in the mixing point were also assumed to model the system. The validity of the plug flow hypothesis for our tubular reactor system was analyzed by checking for axial dispersion and a laminar-flow velocity profile following the criteria recommended by Cutler et al.[29] Axial dispersion was negligible for all the combinations of temperature, pressure and residence time we studied, but the criteria for negligible Poiseuille flow were not completely satisfied for the experiments at 390°C. Cutler et al.[29] determined that random errors from experimental measurement have a larger influence on the errors of the kinetic data than the idealization of tubular reactors to a plug flow behavior. Consequently, we considered that approximation to a plug-flow was also adequate for our experimental system at 390°C. Mixing of the reactant streams has been shown to be a significant factor when the characteristic reaction time tends to be of the same order than the mixing time. Phenix et al.[30] shown in a laboratory-scale tubular reactor constructed with tubing and accessories of the same size we are using that constraining the sectional area of the mixing cross reduced the mixing time from 3.2 to around 0.7 s during the oxidation of methanol in supercritical water at 500°C and 246 bar. Restriction of the sectional area produced higher velocities and Reynolds numbers in the mixing point, thus favoring homogenization of the mixture. This was achieved either by using a specially designed cross with reduced inner diameters, or by inserting the thermocouple deeper into the intersection of a standard cross. The latter was the option we followed in our system. However, data from the experiments at the shortest residence time have larger uncertainty since mixing time and residence time are of the same magnitude. This means that complete mixing is achieved only when DBE has been significantly converted under conditions that clearly deviate from the plug flow hypothesis.

Another simplification we included in the model was that the density of the mixture was considered independent of composition, and was assumed to be that of pure water at the temperature and pressure of reaction. This is a reasonable assumption since a large excess of water was used ($\Theta_W = 100$ $\mathrm{mol_W/mol_{DBE0}}$). In the resulting Eqs 1 to 5, it was also assumed that the thermal scission of the DBE molecule is first-order on DBE concentration, the hydrolysis reaction is first-order on DBE, DBE formation is second-order on BAL concentration and that the degradation of BAL is first-order. Furthermore, the reversible hydrolysis reaction and the benzyl alcohol secondary reactions are assumed to be catalyzed by protons, which are formed from water by dissociation. Equations 6 to 8 express the dependence of their rate constants with the concentration of protons, $C_H^+$. If pure water is used, the concentration of protons is given by Eq. 9 and the ion product of water $K_W$*(mol$^2$/kg$^2$) is calculated from Eq. 10.[31] Water density in Eqs 9 and 10 $\rho_W$ is expressed in kg/L, and it was taken from published data.[32]

$$\frac{dC_{DBE}}{d\tau} = -k_1 C_{DBE} - k_2' C_{DBE} + k_3' C_{BAL}^2 \qquad (1)$$

$$\frac{dC_{BAL}}{d\tau} = 2k_2' C_{DBE} - 2k_3' C_{BAL}^2 - k_4' C_{BAL} \qquad (2)$$

$$\frac{dC_{BZA}}{d\tau} = k_1 C_{DBE} \tag{3}$$

$$\frac{dC_{TOL}}{d\tau} = k_1 C_{DBE} \tag{4}$$

$$C_{DEG} = C_{DBE0} - \left( C_{DBE} + \frac{C_{BAL} + C_{BZA} + C_{TOL}}{2} \right) \tag{5}$$

$$k_2 = \frac{k_2'}{C_{H^+}} \tag{6}$$

$$k_3 = \frac{k_3'}{C_{H^+}} \tag{7}$$

$$k_4 = \frac{k_4'}{C_{H^+}} \tag{8}$$

$$C_{H^+} = \rho_W (K_W^*)^{0.5} \tag{9}$$

$$\log(K_W^*) = -4.098 - \frac{3245.2}{T} + \frac{2.2362 \cdot 10^5}{T^2} - \frac{3.984 \cdot 10^7}{T^3} + \left( 13.957 - \frac{1262.3}{T} + \frac{8.5461 \cdot 10^5}{T^2} \right) \log \rho_W \tag{10}$$

The values of the rate constants $k_1$, $k_2$, $k_3$ and $k_4$ were obtained for each combination of T and P by minimizing the least squares function in Eq. 11

$$OF = \sum_{i=1}^{n} \sum_{j=1}^{m} (f_{ij}^{experimental} - f_{ij}^{model})^2 \tag{11}$$

where n is the number of data points for the experiment (constant $P$, $T$, $C_{DBE0}$ and $\Theta_W$), and m is the number of chemical species $f_{ij} = C_{ij}/C_{DBE0}$

Figures 2 to 6 compare the experimental concentrations and those calculated from the model using the best-fit values for the rate constants, and Figure 5 shows the experimental selectivity toward benzyl alcohol conversion at selected pressures with that calculated from the model. A good agreement is observed for all the experiments, supporting the validity of the reaction model. Figure 8 shows a sensitivity analysis for the influence of the rate constants on the least squares objective function $OF$ for the series at 375°C and 225 bar. This analysis shows that all rate constants were evaluated accurately because the error function $OF$ is very sensitive to their values, except for the rate constant for benzyl alcohol conversion to DBE $k_3$, which has the larger uncertainty. This was because reaction 3 was hindered by the displacement of the equilibrium toward benzyl alcohol due to the extremely high concentration of water that we used in our experiments. The same was observed for the sensitivity analyses developed for experiments at other temperatures and pressures.

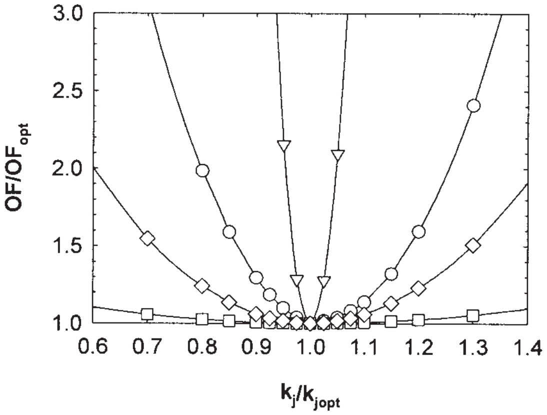

**Figure 8. Sensitivity analysis for the experiment at 375°C and 225 bar ($k_1$ ○; $k_2$ ▽; $k_3$ □; $k_4$ ◇).**

Figure 9 shows the Arrhenius plot for the rate constant of the acid-catalyzed hydrolysis of DBE, $k_2$. The apparent activation energy in the subcritical region was around 160 kJ/mol. The rate constant decreased with water density and it shows an exponential decay with the reduced water density ($\rho_r = \rho/\rho_C$) at $\rho_r > 1$, although the net rate of hydrolysis increased with density since more free protons were available to catalyze the reaction due to water dissociation. According to the transition state theory, this means that the volume of activation of the transition state complex is positive, which suggests that the bond cleavage may proceed trough a $S_N1$-type mechanism. A solvated proton, previously originated by water dissociation, and a DBE molecule form an activated complex ($DBEH^+$) by attachment of the proton to the oxygen atom in ether bond. Then the activated complex undergoes an unimolecular scission to form benzyl alcohol and a $C_6H_5$-$CH_2^+$ cation, which is the rate-limiting step,[33,34] and the latter reacts fast with a water molecule to form benzyl alcohol and a solvated proton. This mechanism is also in agreement with the $S_N1$ mechanism reported for the hydrolysis of diphenylether in supercritical water.[4] The Kirkwood analysis of the influence of the solvent dielectric constant on the rate of hydrolysis shows that there is a linear relationship between $RTln(k_2)$ and $(\varepsilon-1)/\varepsilon$ (Figure 9). The hydrolysis rate constant decreases with the dielectric constant of water, which is characteristic of systems where the transition state complex is less polar than the reactants. Figure 10 shows the values of the rate constant for the acid catalyzed formation of DBE from benzyl alcohol $k_3$. For the experiments performed at 325°C, the best-fit values of $k_3$ were 0.0, since the reaction was practically irreversible at this temperature due to the high excess of water (see Figure 4). However, the values of $k_3$ that we obtained have to be considered only as an indication of its order of magnitude due to the low sensitivity of the least squares function to $k_3$. Since most of the experiments were performed at short reaction time the conversion of DBE did not approach equilibrium sufficiently to obtain precise values of $k_3$. However, some conclusions can be inferred from the analysis of this rate constant. Water density also lowers $k_3$, and the Kirkwood analysis of the dependence of $k_3$ with water dielectric constant shows that the rate of DBE formation decreases with the dielectric constant of the media, with a linear relationship between $RTln(k_3)$ and $(\varepsilon$-$1)/\varepsilon$. The concentration equilibrium constant for the hydrolysis reaction ($K_C = k_2/(C_W k_3)$), also shown in Figure 10, increases with the water density and

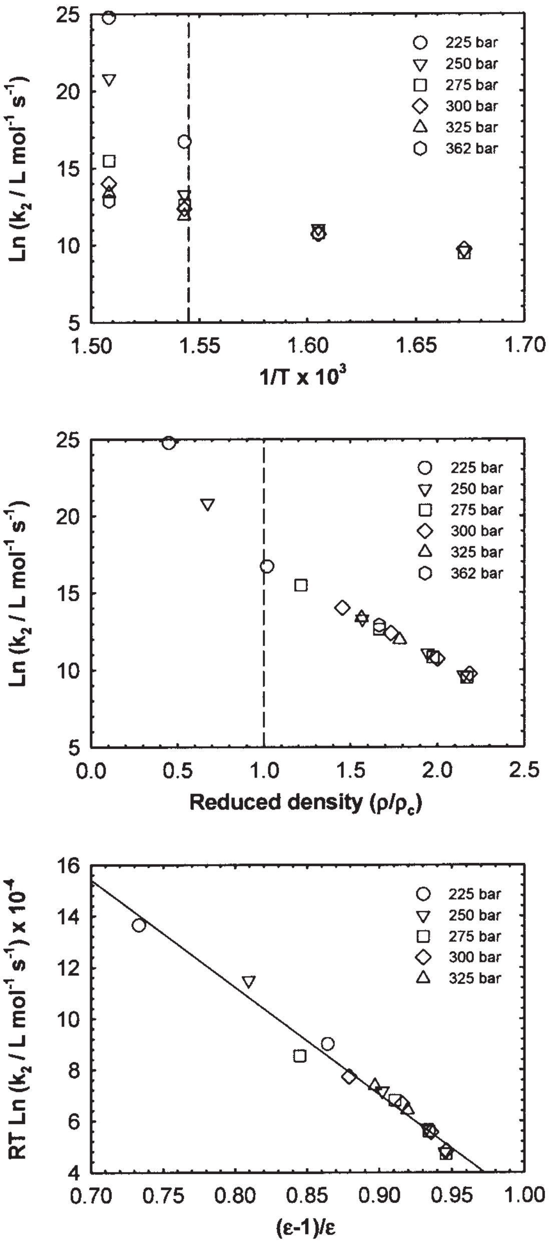

**Figure 9. Dependence of the reaction rate constant $k_2$ on temperature, reduced density and dielectric constant of water.**

the dielectric constant. As the solvent density and polarity raise the reaction rates are lowered, but the equilibrium shifts toward the formation of benzyl alcohol, which is more polar than DBE (1.71 and 1.39 debye, respectively). The dependence of the rate constant for benzyl alcohol decomposition $k_4$, with temperature and pressure is shown in Figure 11. At subcritical temperature the activation energy was close to 170 kJ/mol. Water density and dielectric constant lowered the rate of reaction 4. Kirkwood analysis shows a linear relationship between $RTln(k_4)$ and $(\varepsilon-1)/\varepsilon$, which indicates that the reaction may be catalyzed by free protons as we have assumed in our model. However, it has to be considered that this reaction lumps all processes that are involved in possible ring-opening reactions and the formation of condensation products. None of those products was identified nor quantified, therefore, reaction 4 lacks mechanistic meaning. Finally, Figure 12 plots the values of the rate constant for the thermal cleavage of DBE, $ln(k_1)$, in front of the inverse of the absolute temperature; the apparent activation energy in the subcritical region was 80 kJ/mol. The effect of water density and dielectric constant on the rate of thermal scission were different than for the acid-catalyzed hydrolysis reactions. At $\rho_r < 1$ and $\rho_r > 1.5$ density reduces the rate of thermal scission, but in the interval $(1 < \rho_r < 1.5)$ $k_1$ appears to be independent of the change on water density. The influence of density points to a positive volume of activation for DBE decomposition to benzaldehyde and toluene, which is qualitatively consistent with an unimolecular scission,[35] and agrees with the free-radical reaction pathway proposed by Townsend et al.[28,36] In our model $k_1$ is the overall rate constant of thermal scission and lumps the rates of the individual reaction steps involved in the free-radical mechanism. The dependence of $k_1$ on water density evolves from the combined influence of density on each reaction step. Kirkwood analysis shows that there is not a straight relationship between $RTln(k_1)$ and $(\varepsilon\text{-}1)/\varepsilon$, which supports the nonionic character of this reaction.

### *Effect of NaCl addition*

The addition of inorganic salts such as NaCl to supercritical water increases the ionic strength of the system with little variation in density, and this has been used to gather more evidence on the nature of the transition state complex for

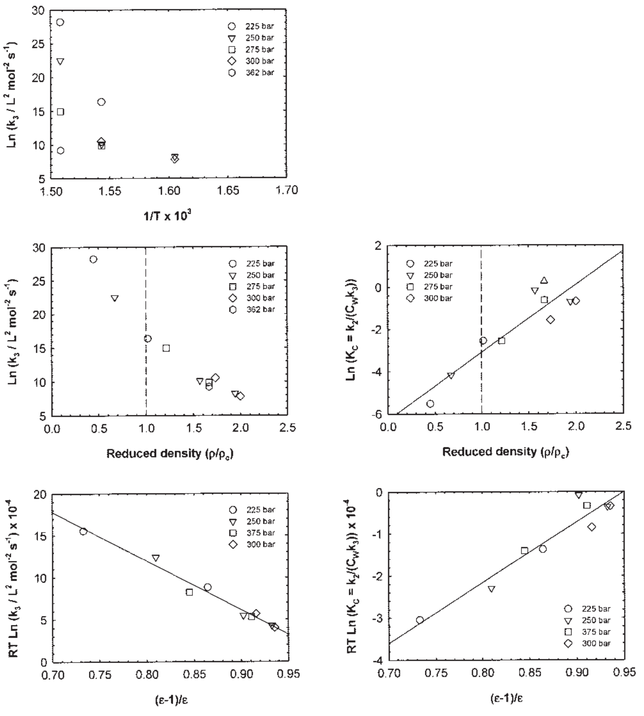

**Figure 10. Dependence of the reaction rate constant $k_3$ on temperature, reduced density and dielectric constant of water, and variation of the concentration equilibrium constant $K_C$ with reduced density and dielectric constant.**

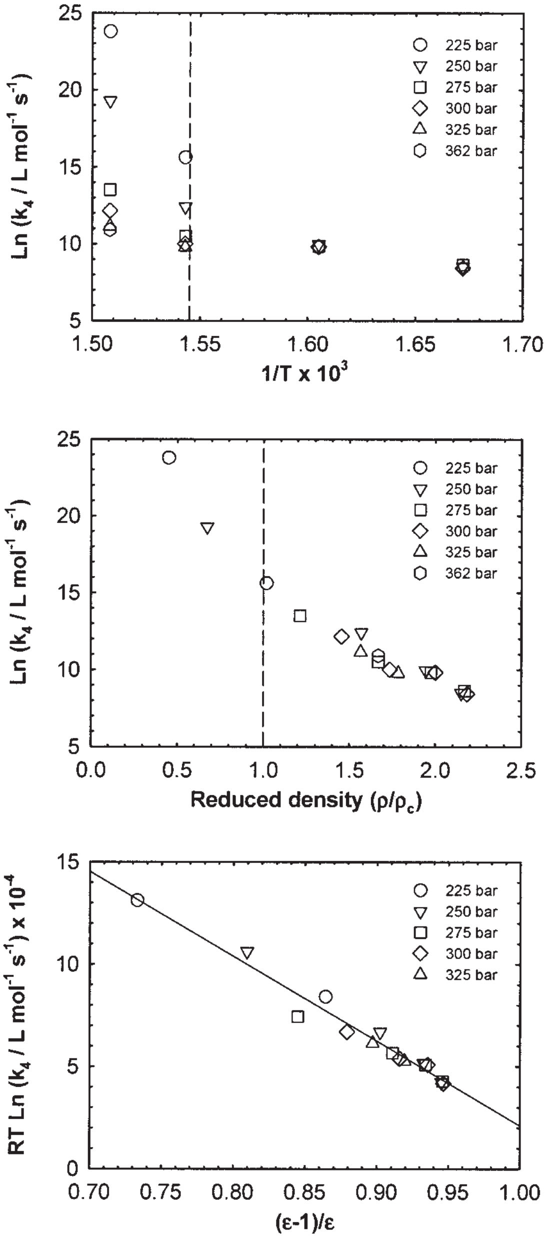

**Figure 11. Dependence of the reaction rate constant $k_4$ on temperature, reduced density and dielectric constant of water.**

several hydrothermolysis reactions conducted in supercritical water.[15,18,37] We conducted experiments at 375°C, 225 bar and a water load, $\Theta_W$, of 100 $mol_{water}/mol_{DBE}$, with the addition of increasing amounts of NaCl (from 3.420 $10^{-2}$ to 5.128 $10^{-1}$ mol/kg) in order to confirm the mechanism that we have proposed for DBE hydrolysis. The critical point for the water - NaCl system at 375.5°C is 223.5 bar, and 0.09% of NaCl (~2.25 $10^{-2}$ mol/kg).[38] Our experiments were performed at a slightly higher pressure and NaCl concentrations above the critical, therefore, we may assume that we were operating in the supercritical region, and that no phase separation did occur during the experiments. This assumption is further supported by the tendency of organic solutes in supercritical water to lower the critical point of the system. The ionic strength of the solvent was calculated with Eq. 12. The concentrations of dissociated sodium and chloride ions were determined from the equilibrium concentrations for the water/NaCl system using the equations for the equilibrium constants given by Lvov et al.[39] and the equation proposed by Marshall and Franck[31] for the ion product of water. The equilibrium concentrations and the ionic strength are reported in Table 1. Figure 13 shows the fractional yields obtained at the different salt concentrations. The addition of 3.420 $10^{-2}$ mol/kg of NaCl reduced the yield of benzyl alcohol to extremely low values and nearly suppressed the formation of degradation products, while the yields of benzaldehyde and toluene doubled with respect to the experiment

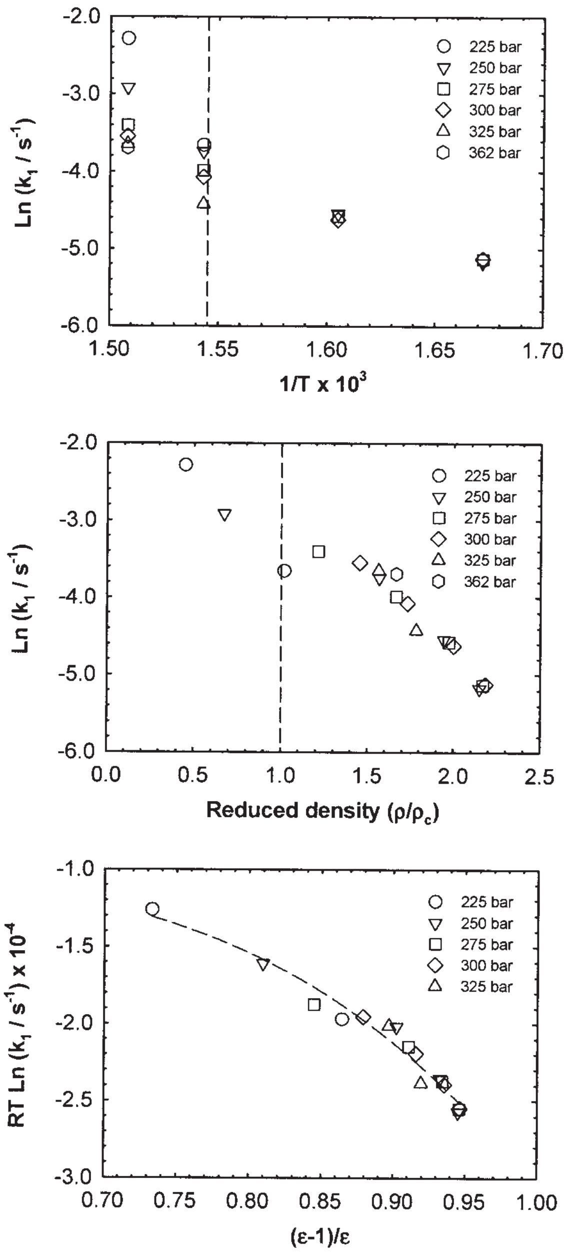

**Figure 12. Dependence of the reaction rate constant $k_1$ on temperature, reduced density and dielectric constant of water.**

**Table 1. Equilibrium Concentrations for NaCl Dissociation Products and Ionic Strength for the Supercritical Water Hydrothermolysis of DBE at 375°C, 225 Bar and $\Theta_W = 100\ \text{mol}_{water}/\text{mol}_{DBE0}$**

| $[NaCl]_0$ (mol/kg) | [NaCl] (mol/kg) | [HCl] (mol/kg) | [NaOH] (mol/kg) | $[H^+]$ (mol/kg) | [OH] (mol/kg) | $[Na^+]$ (mol/kg) | [Cl] (mol/kg) | Ionic Strength |
|---|---|---|---|---|---|---|---|---|
| 0 | 0 | 0 | 0 | $1.745\ 10^{-8}$ | $1.745\ 10^{-8}$ | 0.0 | 0.0 | ~0.0 |
| $3.420\ 10^{-2}$ | $3.035\ 10^{-2}$ | $3.292\ 10^{-6}$ | $3.382\ 10^{-6}$ | $1.298\ 10^{-8}$ | $2.346\ 10^{-8}$ | $3.847\ 10^{-3}$ | $3.847\ 10^{-3}$ | $3.847\ 10^{-3}$ |
| $1.026\ 10^{-1}$ | $9.573\ 10^{-2}$ | $6.021\ 10^{-6}$ | $6.010\ 10^{-6}$ | $1.297\ 10^{-8}$ | $2.348\ 10^{-8}$ | $6.832\ 10^{-3}$ | $6.832\ 10^{-3}$ | $6.832\ 10^{-3}$ |
| $2.393\ 10^{-1}$ | $2.287\ 10^{-1}$ | $9.304\ 10^{-6}$ | $9.294\ 10^{-6}$ | $1.297\ 10^{-8}$ | $2.349\ 10^{-8}$ | $1.056\ 10^{-2}$ | $1.056\ 10^{-2}$ | $1.056\ 10^{-2}$ |
| $5.128\ 10^{-1}$ | $4.972\ 10^{-1}$ | $1.372\ 10^{-5}$ | $1.370\ 10^{-5}$ | $1.296\ 10^{-8}$ | $2.349\ 10^{-8}$ | $1.557\ 10^{-2}$ | $1.557\ 10^{-2}$ | $1.557\ 10^{-2}$ |

without salt addition. The addition of NaCl lowered the concentration of dissociated protons from $1.75\ 10^{-8}$ to $1.30\ 10^{-8}$ mol/kg and reduced the rate of DBE hydrolysis and the yield of benzyl alcohol. The decrease in hydrolysis rate upon addition of small amounts of NaCl was also observed for the hydrolysis of diphenylether (DPE) in SCW at 430°C, and a reduced water density of 1.45 when NaCl concentration was below 0.1 mol/kg.[18] This was attributed to the reduction in the concentration of dissociated protons due to the formation of HCl ion pairs, according to the ionic equilibrium for the water/NaCl system

$$l = \frac{1}{2} \cdot (C_{Na^+} \cdot Z_{Na^+}^2 + C_{Cl^-} \cdot Z_{Cl^-}^2) \tag{12}$$

When the salt concentration was $1.026\ 10^{-1}$ mol/kg the conversion of DBE and the yield of benzyl alcohol increased again, although they were still below the values obtained with pure water. The yields of benzaldehyde, toluene and degradation products were close to those of the previous salt concentration. The concentration of free protons remained constant and the ionic strength of the media almost doubled. Conversion of DBE and yield of benzyl alcohol and other products increased again when the ionic strength was augmented by the use of higher concentrations of added NaCl; when the salt concentration was $5.128\ 10^{-1}$ mol/kg, the conversion of DBE and the yield of products recovered the values obtained with pure water. The concentration of free protons remained constant at around $1.30\ 10^{-8}$ mol/kg in all the range of salt concentrations that we studied. The rate constants of the kinetic model were estimated from the experimental data for each salt concentration. The rate of DBE hydrolysis $k_2$ is shown in Figure 14 as the relationship between $ln(k_2/k_{20})$ and $I^{0.5}$, where $k_{20}$ is the hydrolysis rate constant in pure water, $k_2$ is the rate constant at a certain salt concentration, and $I$ is the ionic strength of the solution calculated with Eq. 12 from the equilibrium concentrations reported in Table 1. The hydrolysis rate constant decreases with the ionic strength of the solution below a salt concentration of around 0.1 $\text{mol}_{NaCl}$/kg, but then it increases again denoting a positive effect of the ionic strength on the hydrolysis rate. This behavior does not agree with the Bronsted-Bjerrum theorem for ionic reactions in solution, from which a linear relationship should be expected. It is worth noticing that this relationship is based on the Debye-Hückel theory that relates the activity coefficients of the reactants and

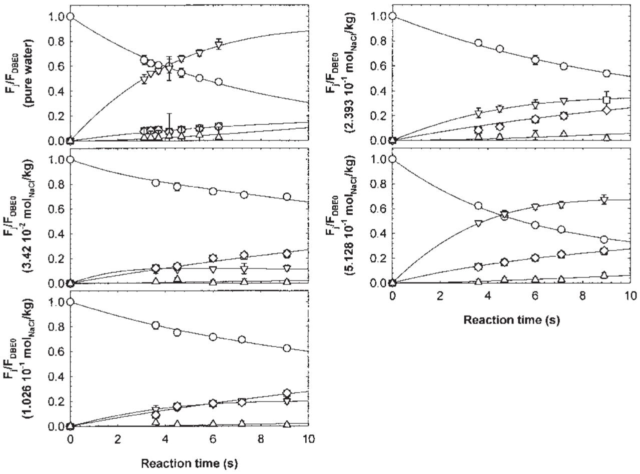

**Figure 13. Hydrothermolysis of DBE at 275°C, 225 bar and $\Theta_W = 100\ \text{mol}_{water}/\text{mol}_{DBE}$ with NaCl addition.**

Fractional yields of reaction products at 0.0, $3.42\ 10^{-2}$, $1.026\ 10^{-1}$, $2.393\ 10^{-1}$, $5.128\ 10^{-1}$ $\text{mol}_{NaCl}$/kg (DBE ○; BAL ▽; BZA □; TOL ◇; DEG △).

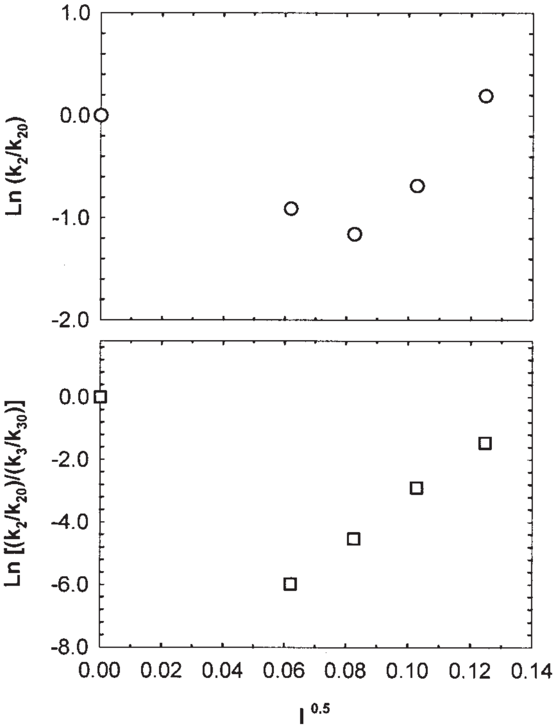

**Figure 14. Hydrothermolysis of DBE at 275°C, 225 bar and $\Theta_W = 100\ \text{mol}_{water}/\text{mol}_{DBE}$ with NaCl addition.**

Variation of the relative rate of hydrolysis $ln(k_2/k_{20})$ and the concentration equilibrium constant $ln[(k_2/k_{20})/(k_3/k_{30})]$ with ionic strength.

the activated complex with the ionic strength of dilute solutions, typically below 0.01 M. Although we are using salt concentrations well above this limit, we have to consider that the degree of dissociation of NaCl in supercritical water is small. According to the equilibrium calculations in Table 1, the higher concentration of dissociated ions was only 1.557 $10^{-2}$ mol/kg (~5.11 $10^{-3}$ mol/L; $\rho_W = 328.19$ kg/m$^3$), which falls in the zone of validity of the theory. The decrease in the rate constant for DBE hydrolysis with ionic strength at low concentrations of NaCl points to a transition state complex that is less polar than the reactants, in concordance with the negative effect of the dielectric constant on the hydrolysis rate constant. A previous study on the effect of NaCl on the hydrolysis of DBE at 380°C and a reduced water density of 0.5 reported at increase on the rate of hydrolysis at salt concentrations above 0.1 M (~0.09 mol/kg), up to around 1.0 M (~0.91 mol/kg).[37] Although we have performed our experiments at a reduced water density of 1.04, the influence of salt addition at a concentration higher than 0.1 mol/kg follows the same trend and raises the rate of DBE hydrolysis. The positive effect of salt addition at a concentration above 0.1 M on the rate of hydrolysis, was also reported for DPE and it was rationalized by a new reaction mechanism that was based on the Lewis acid behavior of the Na$^+$ ion, which generated free protons in the hydration shell of the water clusters surrounding the Na$^+$ ions by charge transfer.[18] Our results confirm that benzyl alcohol is formed from DBE by acid-catalyzed hydrolysis. This reaction is catalyzed by protons in pure supercritical water and also by solvated Na$^+$ ions. The ionic strength of the system also has a strong influence on the concentration equilibrium constant ($k_2/k_3$) for the hydrolysis of DBE. Figure 14 shows that the addition of small amounts of NaCl decreases the relative concentration equilibrium constant $(k_2/k_{20})/(k_3/k_{30})$, but it grows exponentially with $I^{0.5}$ when the concentration of NaCl is augmented due to the change in the activity coefficients of the reactants and products with the ionic strength of the system. The change in activity coefficients caused by the variation in the solvent-solute interactions that arise from salt addition to the system also affects the rate constant of thermal scission of DBE $k_1$, which is shown in Figure 15 as a function of the molal concentration of NaCl. The addition of salt increases the rate of thermal scission of DBE to toluene and benzaldehyde.

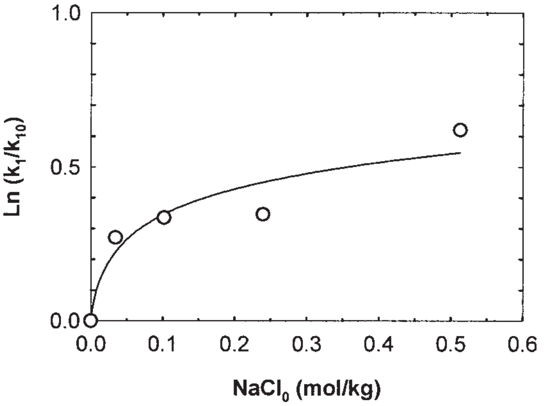

**Figure 15. Hydrothermolysis of DBE at 275°C, 225 bar and $\Theta_W$ = 100 mol$_{water}$/mol$_{DBE}$ with NaCl addition.**

Variation of the rate constant of thermal decomposition of DBE $ln(k_1/k_{10})$ with the concentration of added salt, NaCl$_0$ (mol/kg).

## Conclusions

Dibenzyl ether preferentially undergoes acid-catalyzed hydrolysis in supercritical water to yield benzyl alcohol as reaction product, although this path competes with thermal scission of the ether bond to yield toluene and benzaldehyde. Water density lowers the rate constant for the thermal scission reaction, except for the interval of reduced density from 1.0 to 1.5, where it has little influence. Therefore, conditions that favor an increase in water density reduce the rate of the pyrolysis pathway. The isothermal rate constant for the hydrolysis reaction also decreases with water density showing that the volume of activation for the transition state complex is positive. This is explained by assuming a $S_N1$ mechanism that is rate-limited by the dissociation of the protonated dibenzylether (DBEH$^+$) to form benzyl alcohol and a $C_6H_5\text{-}CH_2^+$ ion, which further reacts with water to form a second molecule of benzyl alcohol. Kirkwood analysis shows a linear relationship between the $RTln(k_2)$ and $(\varepsilon\text{-}1)/\varepsilon$. The dielectric constant lowers the hydrolysis rate constant showing that the transition state complex has a lower dipole moment than the reactants (DBE and H$^+$). This is also in agreement with the reduction in $k_2$ that is observed when the ionic strength of the medium is increased by the addition of a small concentration of NaCl. Although the reaction rate constants for pyrolysis and hydrolysis are both lowered by water density, selectivity toward benzyl alcohol formation is improved because the rate of the hydrolysis pathway is dramatically accelerated due to the increase in the water ion product with water density, which means that more free protons are available to catalyze the reaction. Finally, it appears that the Na$^+$ ions may act as Lewis acids by charge transfer to the water molecules in their hydration shell and can, thus, catalyze the hydrolysis of DBE, as previously proposed by Penninger et al.[18] for DPE hydrolysis.

## Acknowledgments

The authors are indebted to the Catalan Regional Government and the Spanish Government for financial support (projects 2001SGR-00323 and PPQ2001-1215, respectively). G. González is obliged to the Rovira i Virgili University for economic support.

## Literature Cited

1. Shaw RW, Brill TB, Clifford AA, Eckert CA, Franck EU. Supercritical water, a medium for chemistry. *Chem. Eng. News*. 1991;69:26-39.
2. Savage PE, Gopalan S, Mizan TI, Martino CJ, Brock EE. Reactions at supercritical conditions: applications and fundamentals. *AIChE J*. 1995;41:1723-1778.
3. Savage PE. Organic chemical reactions in supercritical water. *Chem. Rev*. 1999;99:603-621.
4. Penninger JML, Kersten RJA, Baur HCL. Reactions of diphenylether in supercritical water - mechanism and kinetics. *J. Supercrit. Fluids*. 1999;16:119-132.
5. Sasaki M, Kabeyemela B, Malaluan R, Hirose S, Takeda N, Adschiri T, Arai K. Cellulose hydrolysis in subcritical and supercritical water. *J. Supercrit. Fluids*. 1998;13:261-268.
6. Kabeyemela BM, Adschiri T, Malaluan RM, Arai K. Kinetics of glucose epimerization and decomposition in subcritical and supercritical water. *Ind. Eng. Chem. Res*. 1997;36:1552-1558.
7. Kabeyemela BM, Adschiri T, Malaluan RM, Arai K. Degradation

kinetics of dihydroxyacetone and glyceraldehyde in subcritical and supercritical water. *Ind. Eng. Chem. Res*. 1997;36:2025-2030.

8. Kabeyemela BM, Adschiri T, Malaluan RM, Arai K, Ohzeki H. Rapid and selective conversion of glucose to erythrose in supercritical water. *Ind. Eng. Chem. Res*. 1997;36:5063-5067.
9. Kabeyemela BM, Takigawa M, Adschiri T, Malaluan RM, Arai K. Mechanism and kinetics of cellobiose decomposition in sub- and supercritical water. *Ind. Eng. Chem. Res*. 1998;37:357-361.
10. Holgate HR, Meyer JC, Tester JW. Glucose hydrolysis and oxidation in supercritical water. *AIChE J*. 1995;37:637-648.
11. Yu D, Aihara M, Antal MJ. Hydrogen production by steam reforming glucose in supercritical water. *Energy Fuels*. 1993;37:574-577.
12. Minowa T, Fang Z. Hydrogen production from cellulose in hot compressed water using reduced nickel catalyst: product distribution at different reaction temperatures. *J. Chem. Eng. Jpn*. 1998;31:488-491.
13. Xu X, Matsumura Y, Stenberg J, Antal MJ. Carbon-catalyzed gasification of organic feedstocks in supercritical water. *Ind. Eng. Chem. Res*. 1996;35:2522-2530.
14. Schmieder H, Abeln J, Boukis N, Dinjus E, Kruse A, Kluth M, Petrich G, Sadri E, Schacht M. Hydrothermal gasification of biomass and organic wastes. *J. Supercrit. Fluids*. 2000;17:145-153.
15. Huppert GL, Wu BC, Townsend SH, Klein MT, Paspek SC. Hydrolysis in supercritical water: identification and implications of a polar transition state. *Ind. Eng. Chem. Res.* 1989;28:161-165.
16. Lawson JR, Klein MT. Influence of water on guaiacol pyrolysis. Ind. Eng. Chem. Fundam. 1985;24:203-208.
17. Martino CJ, Savage PE. Oxidation and thermolysis of methoxy-, nitro-, and hydroxy-substituted phenols in supercritical water. *Ind. Eng. Chem. Res*. 1999;38:1784-1791.
18. Penninger JML, Kersten RJA, Baur HCL. Hydrolysis of diphenylether in supercritical water. Effects of dissolved NaCl. *J. Supercrit. Fluids*. 2000;17:215-226.
19. Klein MT, Torry LA, Wu BC, Townsend SH, Paspek, SC. Hydrolysis in supercritical water: solvent effects as a probe of the reaction mechanism. *J. Supercrit. Fluids*. 1991;3:222-227.
20. Funazukuri T, Serikawa RS, Yamamura K. Rate of dibenzyl ether decomposition in supercritical water. *Fuel*. 1997;76:865-870.
21. Taylor JD, Steinfeld JI, Tester JW. Experimental measurement of the rate of methyl tert-butyl ether hydrolysis in sub- and supercritical water. *Ind. Eng. Chem. Res*. 2001;40:67-74.
22. Taylor JD, Pacheco FA, Steinfeld JI, Tester JW. Multiscale reaction pathway analysis of methyl tert-butyl ether hydrolysis under hydrothermal conditions. *Ind. Eng. Chem. Res*. 2002;41:1-8.
23. Akiya N, Savage P. Roles of water for chemical reactions in high-temperature water. *Chem. Rev*. 2002;102:2725-2750.
24. Krammer P, Vogel H. Hydrolysis of esters in subcritical and supercritical water. *J. Supercrit. Fluids*. 2000;16:189-206.
25. Xu X, Antal MJ, Anderson, DGM. Mechanism and temperature-dependent kinetics of the dehydration of tert-butyl alcohol in hot compressed liquid water. Ind. *Eng. Chem. Res.* 1997;36:23-41.
26. Antal MJ Jr., Carlsson M, Xu X, Anderson DGM. Mechanism and kinetics of the acid-catalyzed dehydration of 1- and 2-propanol in hot compressed liquid water. *Ind. Eng. Chem. Res*. 1998;37:3820-3829.
27. González G, Salvadó J, Montané D. Reactions of vanillic acid in sub- and supercritical water. *J. Supercrit. Fluids*. 2004;31:57–66.
28. Townsend SH, Abraham MA, Huppert GL, Klein MT, Paspek SC. Solvent effects during reactions in supercritical water. *Ind. Eng. Chem. Res.* 1988;27:143-149.
29. Cutler AH, Antal MJ, Jones M. A critical evaluation of the plug-flow idealization of tubular-flow reactor data. *Ind. Eng. Chem. Res*. 1988; 27,691-697.
30. Phenix BD, DiNaro JL, Tester JW, Howard JB, Smith KA. The effects of mixing and oxidant choice on laboratory-scale measurements of supercritical water oxidation kinetics. *Ind. Eng. Chem. Res*. 2002;41: 624-631.
31. Marshall WL, Franck EU. Ion product of water substance, 0-1000°C, 1-10000 bars. New international formulation and its background. *J. Phys. Chem. Ref. Data*. 1981;10:295-304.
32. Wagner W, Kruse A. Properties of Water and Steam. The Industrial Standard IAPWS-IF97 for the Thermodynamic Properties and Supplementary Equations for Other Properties. Berlin: Springer, 1998.
33. Morrison RT, Boyd RN. Organic Chemistry. Englewood Cliffs (NJ): Prentice-Hall, Inc., 1992.
34. Solomons TWG, Fryhle CB. Organic Chemistry. New York: John Wiley & Sons, Inc., 2000.
35. Luft G, Mehrling P, Seidl H. Decomposition of polymerization initiators under high pressures. *Angew. Makromol. Chem*. 1978;73:95-111.
36. Townsend SH, Klein MT. Dibenzyl ether as a probe into the supercritical fluid solvent extraction of volatiles from coal with water. *Fuel*. 1985;64:635-638.
37. Torry LA, Kaminsky R, Klein MT, Klotz MR. The effect of salts on hydrolysis in supercritical and near-critical water: reactivity and availability. *J. Supercrit. Fluids*. 1992;5:163-168.
38. Bischoff JL, Pitzer KS. Liquid-vapor relations for the system NaCl-$H_2O$: summary of the P-T-x surface from 300 to 500°C. *Am. J. Sci*. 1989;289:217-248.
39. Lvov SN, Zhou XY, Ulyanov SM, Bandura AV. Reference systems for assessing viability and accuracy of pH sensors in high temperature subcritical and supercritical aqueous solutions. *Chemical Geology*. 2000;167:105-115.

*Manuscript received Feb. 27, 2004, and revsion received July 6, 2004.*